Electronic Supplementary Material (ESI) for Soft Matter.
This journal is © The Royal Society of Chemistry 2019

SUPPORTING INFORMATION

Surface Heterogeneity Affects Percolation and Gelation of Colloids: Dynamic Simulations with Random Patchy Spheres

Gang Wang[1] and James W. Swan[*,1]

[1]Department of Chemical Engineering, Massachusetts Institute of Technology, Cambridge, MA
E-mail: jswan@mit.edu

March 20, 2019

1 Brownian Dynamics of Rigid Composite-bead Particles

The mobility problem for rigid composite-bead particles takes the general form:

$$\mathcal{U} = \left(\boldsymbol{\Sigma} \cdot \mathcal{M}^{-1} \cdot \boldsymbol{\Sigma}^T\right)^{-1} \cdot \mathcal{F}, \tag{1}$$

where $\mathcal{F}$ represents a combined the force and torque (including Brownian, inter-particle, and strain contributions) and $\mathcal{U}$ represents a combined translational velocity and angular velocity. Although it is feasible to solve this linear system of equations using nested iterative method, transforming this form into a saddle point problem is a more efficient approach:

$$\begin{bmatrix} \mathcal{M} & \boldsymbol{\Sigma}^T \\ \boldsymbol{\Sigma} & \mathbf{0} \end{bmatrix} \cdot \begin{bmatrix} \mathbf{f} \\ -\mathcal{U} \end{bmatrix} = \begin{bmatrix} \mathbf{0} \\ \mathcal{F} \end{bmatrix}. \tag{2}$$

In order to reduce the number of expensive inversion operations further the Brownian and strain contributions to $\mathcal{F}$ can be represented in an equivalent form:

$$\begin{bmatrix} \mathcal{M} & \boldsymbol{\Sigma}^T \\ \boldsymbol{\Sigma} & \mathbf{0} \end{bmatrix} \cdot \begin{bmatrix} \mathbf{f} \\ -\mathcal{U} \end{bmatrix} = \begin{bmatrix} -\mathbf{K}' \cdot \mathbf{e} - \mathbf{u}^B \\ \mathcal{F}^P \end{bmatrix}, \tag{3}$$

where $\mathcal{F}^P$ only includes the deterministic inter-particle contribution to the force and torque. This approach requires one inversion per time step to determine the particle velocity which can be performed using preconditioned iterative methods such as GMRES. Each iteration of such a method requires a single mobility $\mathcal{M}$ evaluation, which is the most expensive calculation in the algorithm.

An efficient preconditioner for the saddle point problem is:

$$\begin{bmatrix} 6\pi\eta_s a \left[\mathbf{I} - \boldsymbol{\Sigma}^T \cdot \left(\boldsymbol{\Sigma} \cdot \boldsymbol{\Sigma}^T\right)^{-1} \cdot \boldsymbol{\Sigma}\right] & \boldsymbol{\Sigma}^T \cdot \left(\boldsymbol{\Sigma} \cdot \boldsymbol{\Sigma}^T\right)^{-1} \\ \left(\boldsymbol{\Sigma} \cdot \boldsymbol{\Sigma}^T\right)^{-1} \cdot \boldsymbol{\Sigma} & -\frac{1}{6\pi\eta_s a}\left(\boldsymbol{\Sigma} \cdot \boldsymbol{\Sigma}^T\right)^{-1} \end{bmatrix}. \tag{4}$$

This preconditioner does not require any mobility $\mathcal{M}$ evaluation, and can be implemented trivially. When applied to the saddle point matrix, it yields a block triangular matrix that is well-conditioned:

$$\begin{aligned} &\begin{bmatrix} 6\pi\eta_s a \left[\mathbf{I} - \boldsymbol{\Sigma}^T \cdot \left(\boldsymbol{\Sigma} \cdot \boldsymbol{\Sigma}^T\right)^{-1} \cdot \boldsymbol{\Sigma}\right] & \boldsymbol{\Sigma}^T \cdot \left(\boldsymbol{\Sigma} \cdot \boldsymbol{\Sigma}^T\right)^{-1} \\ \left(\boldsymbol{\Sigma} \cdot \boldsymbol{\Sigma}^T\right)^{-1} \cdot \boldsymbol{\Sigma} & -\frac{1}{6\pi\eta_s a}\left(\boldsymbol{\Sigma} \cdot \boldsymbol{\Sigma}^T\right)^{-1} \end{bmatrix} \cdot \begin{bmatrix} \mathcal{M} & \boldsymbol{\Sigma}^T \\ \boldsymbol{\Sigma} & \mathbf{0} \end{bmatrix} \\ &= \begin{bmatrix} 6\pi\eta_s a \left[\mathcal{M} - \boldsymbol{\Sigma}^T \cdot \left(\boldsymbol{\Sigma} \cdot \boldsymbol{\Sigma}^T\right)^{-1} \cdot \boldsymbol{\Sigma} \cdot \left(\mathcal{M} - \frac{1}{6\pi\eta_s a}\mathbf{I}\right)\right] & \mathbf{0} \\ \left(\boldsymbol{\Sigma} \cdot \boldsymbol{\Sigma}^T\right)^{-1} \cdot \boldsymbol{\Sigma} \cdot \left(\mathcal{M} - \frac{1}{6\pi\eta_s a}\mathbf{I}\right) & \mathbf{I} \end{bmatrix}. \end{aligned} \tag{5}$$

When evaluating the stress, we split the Brownian contribution from the hydrodynamic and inter-particle parts, which can computed as:

$$\boldsymbol{\sigma}^H + \boldsymbol{\sigma}^P = -\frac{1}{V}\sum_N \left(\mathbf{x}\mathbf{F}^P + \mathbf{K} \cdot \mathbf{f}^d\right), \tag{6}$$

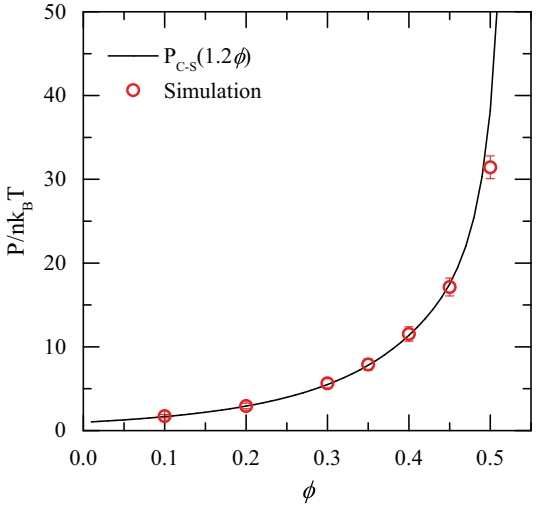

Figure S1: Osmotic pressure comparison between simulation and theoretical prediction by Carnahan-Starling equation with equivalent volume fraction of $\phi_{\text{eff}} = 1.2\phi$.

where $\mathbf{f}^d$ satisfies:

$$\begin{bmatrix} \mathcal{M} & \mathbf{\Sigma}^T \\ \mathbf{\Sigma} & \mathbf{0} \end{bmatrix} \cdot \begin{bmatrix} \mathbf{f}^d \\ -\mathcal{U} \end{bmatrix} = \begin{bmatrix} -\mathbf{K}' \cdot \mathbf{e} \\ \mathcal{F}^P \end{bmatrix}. \tag{7}$$

This calculation requires an additional inversion of the saddle point problem but reduces entirely the noise in the calculation of these contributions to the stress.

The stochastic drift $\nabla \cdot \mathbf{M}^{\mathcal{UF}}$ and Brownian stress $\nabla \cdot \left(\mathbf{R}^{\mathbf{S}\mathcal{U}} \cdot \mathbf{M}^{\mathcal{UF}}\right)$ are challenging to compute in Brownian dynamics simulations [1], where the superscripts indicate the blocks of mobility and resistance tensor respectively. In the present work, we use the random finite difference scheme described in [4, 5] to evaluate these contributions. In this scheme, a random vector $\boldsymbol{\psi}$ with zero mean and covariance satisfying $\langle \psi_i \psi_j \rangle = \delta_{ij}$ is generated. A divergence term $\mathbf{d}$, either $\nabla \cdot \mathbf{M}^{\mathcal{UF}}$ or $\nabla \cdot \left(\mathbf{R}^{\mathbf{S}\mathcal{U}} \cdot \mathbf{M}^{\mathcal{UF}}\right)$, is then evaluated as:

$$d_m = \frac{1}{\lambda} \sum_n \left(B_{mn}(x_i + \lambda \psi_i)\psi_n - B_{mn}(x_i)\psi_n \right), \tag{8}$$

where matrix $\mathbf{B}$ is either $\mathbf{M}^{\mathcal{UF}}$ or $\mathbf{R}^{\mathbf{S}\mathcal{U}} \cdot \mathbf{M}^{\mathcal{UF}}$ depending on which term $\mathbf{d}$ represents, and $\mathbf{x}$ is the position at the current time step. This means the linear transformation $\mathbf{B}$ is evaluated at two positions: $\mathbf{x}$ and $\mathbf{x} + \lambda\boldsymbol{\psi}$, and operated on the same random vector $\boldsymbol{\psi}$. The scale λ measures the step size of the finite difference. With small enough step size, the expression can be approximated as:

$$d_m = \sum_n \frac{1}{\lambda} \left(\lambda \psi_i\right) \partial_i B_{mn}(x_i)\psi_n = \partial_i B_{mn}(x_i) \left(\psi_i \psi_n\right). \tag{9}$$

Thus, the ensemble average of $\mathbf{d}$ is:

$$\langle d_m \rangle = \sum_i \partial_i B_{mi}, \tag{10}$$

where $\partial_i B_{mi}$ is the divergence of matrix $\mathbf{B}$.

2 Volume Fraction Definitions

Volume fraction ϕ used in the article is based on the hydrodynamic radius of composite-bead particles since it is well-defined with the single particle mobility. Thermodynamics also depends on the excluded volume of each particle, which is related to the interactions between beads. Hard-sphere repulsion is usually desired, but due to the absence of a perfect hard-sphere force field for composite-bead particles, certain softness is inevitable.

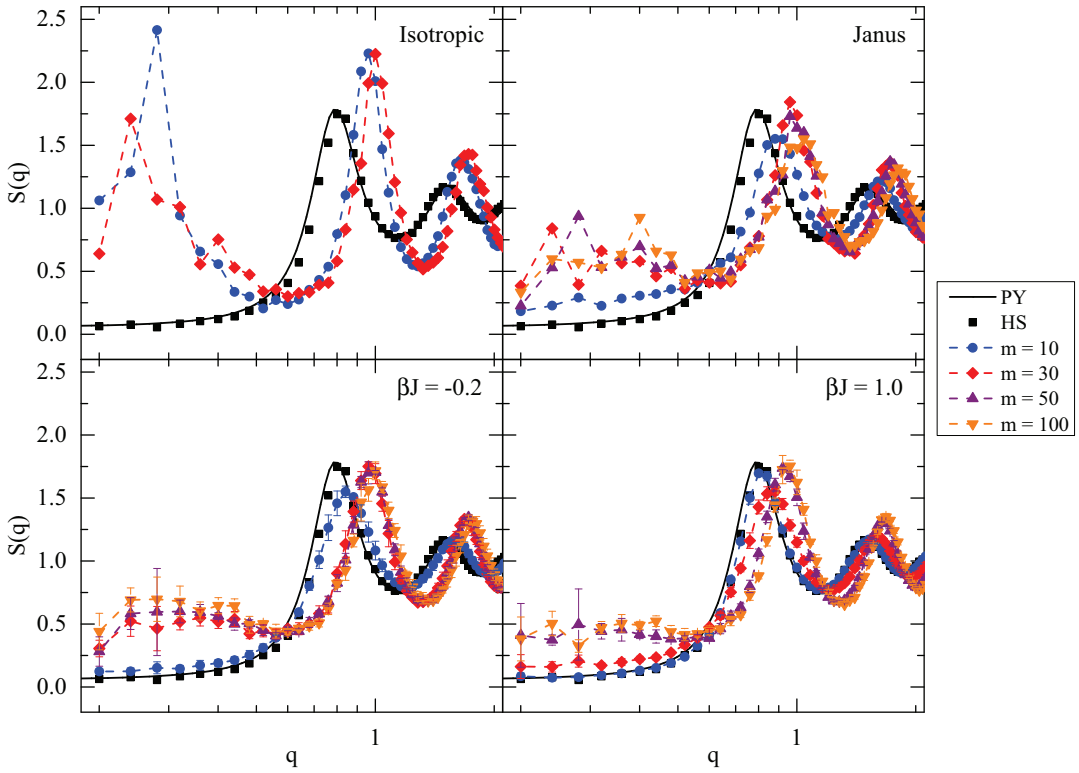

Figure S2: Structure factors of various types of particles with volume fraction $\phi = 0.30$. PY: hard-sphere structure factor predicted by Percus-Yevick theory [6, 7]; HS: structure factor with only parabolic repulsion ($m = 0$). m value is defined as the dimensionless interaction strength: $m = E_Y/k_BT$.

In the present work, a parabolic repulsive interaction is imposed between beads to represent excluded volume effect:

$$E_R(r) = A_R \left(\frac{r}{a_B} - 2 \right)^2, \tag{11}$$

where the energy constant $A_R = 25k_BT$. The equivalent volume fraction based on excluded volume is determined by computing the osmotic pressure with only this potential (without the site-site Yukawa potential), as shown in figure S1. The solid line represents the osmotic pressure predicted by Carnahan-Starling equation:

$$\frac{P_{\text{C-S}}}{nk_BT} = 1 + 4\phi_{\text{eff}} \frac{1 - \frac{1}{2}\phi_{\text{eff}}}{(1 - \phi_{\text{eff}})^3}, \tag{12}$$

with equivalent volume fraction $\phi_{\text{eff}} = 1.2\phi$. It is observed that the osmotic pressure by simulation matches perfectly with the theoretical prediction with 20% higher volume fraction. It can also be concluded that the thermodynamics is better described by the equivalent volume fraction than the volume fraction ϕ based on hydrodynamic radius. Therefore, in this article, equivalent volume fraction is used to compare the simulation results with thermodynamic theories for adhesive hard-spheres.

3 Structure Factor

Figure S2 shows the structure factors, $S(q)$, of various types of particles at $\phi = 0.30$. The result well supports the conclusions in the article. As the interaction strength increases, particles form more bonds with each other, and $S(q)$ at low q becomes higher. However, only the isotropic particle suspension exhibits a peak at low q, indicating long-range spatial correlation, while all the patchy particle suspensions only have moderate increase at low q without any peak. This observation agrees

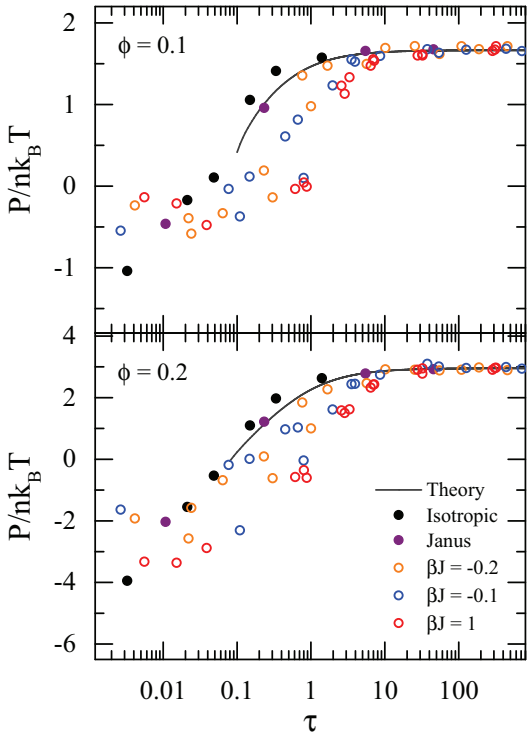

Figure S3: Osmotic pressure P normalized by nk_BT as a function of Baxter temperature τ with volume fractions of 0.10 and 0.20. The prediction from Percus-Yevick theory by Baxter [2] is shown as the solid lines.

with the bond number results in the article, where isotropic attractive particles form 6 nearest neighbors (closed packed clusters) and patchy particles only have 4 (arrested fractal network).

4 Thermodynamics with Other Volume Fractions

Osmotic pressure results at lower volume fractions 0.10 and 0.20 as a function of Baxter temperature τ and a function of average number of bonds $\langle N_b \rangle$ are shown in figure S3 and figure S4, respectively. As expected, the behavior is very similar with the case with volume fraction of 0.30: Baxter temperature cannot give a successful prediction of osmotic pressure while a universal correlation is observed between micro-structure and osmotic pressure regardless of particle type.

References

[1] Banchio, A. J., and J. F. Brady, "Accelerated Stokesian dynamics: Brownian motion," J. Chem. Phys. **118**, 10323–10332 (2003).

[2] Baxter, R. J., "Percus-Yevick equation for hard spheres with surface adhesion," J. Chem. Phys. **49**, 2770–2774 (1968).

[3] Chiew, Y. C., and E. D. Glandt, "Percolation behaviour of permeable and of adhesive spheres," J. Phys. A **16**, 2599–2608 (1983).

[4] Delong, S., F. Balboa Usabiaga, R. Delgado-Buscalioni, B. E. Griffith, and A. Donev, "Brownian dynamics without Green's functions," J. Chem. Phys. **140**, 134110 (2014).

[5] Delong, S., F. Balboa Usabiaga, and A. Donev, "Brownian dynamics of confined rigid bodies," J. Chem. Phys. **143**, 144107 (2015).

[6] Regnaut, C., and J. C. Ravey, "Application of the adhesive sphere model to the structure of colloidal suspensions," J. Chem. Phys. **91**, 1211–1221 (1989).

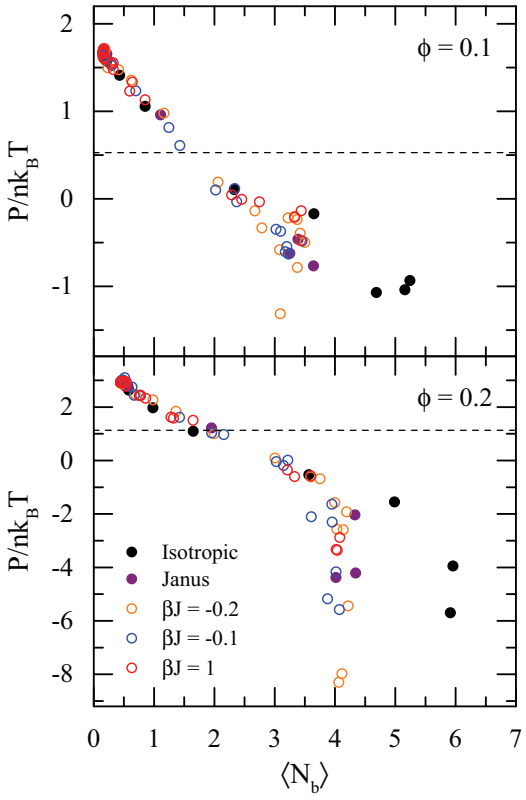

Figure S4: Normalized osmotic pressure P/nk_BT as a function of average number of bonds $\langle N_b \rangle$ with volume fractions of 0.10 and 0.20. The dashed lines are the theoretical percolation osmotic pressures using Percus-Yevick theory [2, 3].

[7] Regnaut, C., and J. C. Ravey, "Erratum: Application of the adhesive sphere model to the structure of colloidal suspensions [J. Chem. Phys. 91, 1211 (1989)]," J. Chem. Phys. **92**, 3250–3250 (1990).